Title	Topological features of lithium disilicate glass-ceramics uncovered through materials informatics
Author(s)	Yamaguchi, Satoshi; Li, Hefei; Funayama, Naoya et al.
Citation	Dental Materials. 2025
Version Type	VoR
URL	https://hdl.handle.net/11094/102882
rights	This article is licensed under a Creative Commons Attribution 4.0 International License.
Note	

ELSEVIER

Topological features of lithium disilicate glass-ceramics uncovered through materials informatics

Satoshi Yamaguchi [a,b,*] , Hefei Li [b], Naoya Funayama [b] , Tomoki Kohno [b], Satoshi Imazato [b,c]

[a] AI Research Unit, Graduate School of Dentistry, The University of Osaka, 1-8 Yamadaoka, Suita, Osaka 565-0871, Japan
[b] Joint Research Laboratory of Advanced Functional Materials Science, Graduate School of Dentistry, The University of Osaka, 1-8 Yamadaoka, Suita, Osaka 565-0871, Japan
[c] Department of Dental Biomaterials, Graduate School of Dentistry, The University of Osaka, 1-8 Yamadaoka, Suita, Osaka 565-0871, Japan

ARTICLE INFO

ABSTRACT

Objective: The aim of this study was to inversely predict the topological features underlying SEM images from arbitrary biaxial flexural strengths of glass-ceramics by Materials Informatics (MI) approach.
Methods: The scanning electron microscopic (SEM) image and in vitro biaxial flexural strength of 10 commercially available/experimental glass-ceramics were collected. The total of 200 SEM images were prepared as input data. Topological features underlying the SEM images were extracted using persistent homology analysis and compressed using principal component analysis. Gaussian mixture regression was employed to develop a machine learning model for predicting biaxial flexural strength based on the topological features. Arbitrary biaxial flexural strengths (390, 411, 442, 478, 515, 564, 597, 610, and 640 MPa) were defined, and an inverse analysis was conducted with the constructed machine learning model to overlay topological features onto SEM images.
Results: The topological features were compressed into 18 principal components. The machine learning model was selected and optimized based on the Bayesian Information Criterion. Using the constructed machine learning model, the biaxial flexural strengths were predicted with a test score of 72 % (Root Mean Squared Error: 53.5, Mean Absolute Error: 40.3). From the arbitrary biaxial flexural strengths, topological features were inversely predicted and overlaid onto SEM images.
Conclusion: The inverse analysis established in this study successfully predicted the topological features on SEM images of glass-ceramics from the biaxial flexural strengths. The MI approach with the inverse analysis promises to make the process to develop glassceramics more time-efficient than the conventional in vitro approach

1. Introduction

New generation of lithium disilicate glass-ceramics, IPS e.max CAD, has been introduced to facilitate the computer-aided design/computer-aided manufacturing (CAD/CAM) milling process since 2006 [1]. In recent years, these lithium disilicate glass-ceramics have been widely used for veneers, inlays, onlays, and single crowns due to their superior translucency, wide range of color shades, and ease of fabrication [2–4]. However, their flexural strengths (210 ± 35–624 ± 106 MPa [4]) are still not enough compared to those of zirconia (467.5 ± 97.5 MPa ~ 898.0 ± 188.5 MPa [5]). Enhancing the flexural strength of these ceramics could potentially expand clinical applications.

Lithium disilicate glass-ceramics consist of two phases: a crystalline phase containing approximately 65 % lithium disilicate and a glass matrix [4]. Enhancing the mechanical properties of these materials is influenced by various factors, with microstructure playing a particularly significant role [3,6]. The conventional experimental approach to modifying the microstructure involves controlling the compositions of different phases and optimizing the heating process to achieve the desired crystallinity [7]. By adjusting these parameters, experimental blocks are fabricated and subsequently subjected to mechanical testing. ISO 6872: 2015 standard recommends conducting biaxial flexural strength test. However, these ceramics tend to have surface flaws and cracks during fabrication, including machining damage from CAD/CAM process [8,9]. Thus, the conventional experimental approach, which relies on repetitive testing, is time-consuming due to the challenges associated with specimen preparation.

In recent years, the demand for accelerating materials modification

and development has driven significant advancements in materials informatics (MI), which is defined as the application of computational methodologies to address challenges inherent in materials science [10]. The integration of machine learning (ML) with experimental datasets has transformed the traditional trial-and-error approach into a data-driven paradigm [11]. A typical workflow for integrating ML into materials research consists of three key components: a well-organized materials dataset, an appropriate ML algorithm, and a clearly defined research problem involving target materials that can benefit from ML techniques. A crucial step in this process is preprocessing the raw materials database into a format compatible with the ML model's input structure, such as vectors, while effectively capturing the essential features of the materials. This preprocessing phase requires expertise in materials science along with a strong understanding of ML models to ensure high accuracy and efficiency in addressing complex materials challenges [12]. The importance of MI has steadily grown to predict material properties across various materials such as organic, inorganic, and composite materials [13–15].

In the field of dental materials, literatures on the application of MI are still limited. The MI approach has been applied to predict the flexural strength of CAD/CAM resin composites [16] and performance outcomes of direct resin composites [17]. However, this study primarily focuses on the direct analysis or prediction of the target properties, using compositional or structural information as inputs and material properties as the outputs [18]. Through this forward process, although optimal designs that surpass those in the training dataset can be proposed, it is not feasible to identify specific optimal designs or regions that fall within the predefined boundary conditions, such as strength [19]. To overcome this limitation, an inverse ML framework may be useful. Unlike forward ML, inverse analysis aims to predict internal structural information based on the desired properties.

Scanning electron microscopy (SEM) has been widely used as characterization method for observing and analyzing the internal structures of ceramics. However, quantifying these differences remains challenging due to variations in crystal sizes, shapes, and distributions among different products. Recently, a suite of techniques known as topological data analysis (TDA) has shown significant potential for extracting meaningful information from such complex images. TDA examines topological invariants, which are global intrinsic structure properties such as connected components, circles, rings, loops, channels, cavities, and voids [20,21]. TDA encompasses a range of methods inspired by algebraic topology, with persistent homology (PH) serving as a fundamental tool. While geometric approaches to data analysis have historical roots, TDA has established itself as a distinct field, largely due to the pioneering works of Edelsbrunner et al. and Zomorodian and Carlsson in PH [22,23]. PH enables the topological simplification of complex data across different spatial resolutions, allowing intrinsic topological invariants to be extracted from images. It represents these extracted topological features using a persistent diagram. This technique has already been applied in various fields such as the extraction of multiscale topological features from biomolecular structures, the analysis of CT image data to identify crack formation trigger sites in iron, and the investigation of structural variations in isotropic and anisotropic sodium silicate glasses, among other applications [21,24,25].

The aim of this study was to develop a framework utilizing a MI approach to both directly predict the biaxial flexural strengths of lithium disilicate glass-ceramics from SEM images and inversely predict the internal topological features underlying these SEM images based on predefined biaxial flexural strength values.

2. Materials and methods

2.1. Experimental and commercial lithium disilicate glass-ceramics

Nine commercially available lithium disilicate glass-ceramics and one experimental lithium disilicate glass-ceramic were considered: Celtra Duo (Lot: 16001012, Dentsply Sirona, Charlotte, NC, USA), CEREC Tessera (Lot: 16009642, Dentsply Sirona), IPS e.max CAD (Lot: Y08938, Ivoclar, Schaan, Liechtenstein, Switzerland), IPS e.max Press (Lot: X49004, Ivoclar), Initial LiSi Block (Lot: 2010121, GC Corp., Bunkyo, Tokyo, Japan), Initial LiSi Press (Lot: 1806021, GC Corp.), N!ce (Lot: NJ372, Straumann, Basel, Switzerland), Vita Sprinity (Lot: 36211, Vita Zahnfabrik, Bad Säckingen, Germany), Vintage Prime Press (Lot: 0521101, Shofu, Kyoto, Japan), and LH052 (Lot: 211222, GC R&D Corp., Itabashi, Tokyo).

2.2. Specimen preparation

Disk-shaped specimens with a diameter of 12 mm were fabricated using a milling machine (Aadva LW-I, GC Corp., Japan) and sectioned to a thickness of 2.4 mm using a diamond-coated precision sectioning blade (ISOMET2000, Buehler, Illinois, USA). CEREC Tessera specimens underwent heat treatment in a furnace according to the manufacturer's recommendation, while IPS e.max CAD specimens were crystallized using a furnace following the manufacturer's guidelines. All specimens were then polished to a final thickness of 1.2 ± 0.2 mm. For the LiSi block, N!ce, Celtra Duo, and LH052, polishing was performed after milling without additional heat treatment or crystallization. The CAD/CAM glass-ceramics were tested with a sample size of n = 6, while the pressed ceramics were tested with n = 12.

2.3. Biaxial flexural strength test and scanning electron microscope analysis

According to the ISO 6872: 2015 standard, a custom-made piston-on-three-balls (P3B) biaxial fixture was prepared. Each specimen was supported by three stainless-steel ball bearings with a diameter of 4.5 ± 0.1 mm, positioned $120°$ apart on a support circle with a diameter of 11 mm. A flat piston with a diameter of 1.4 mm was applied at the center of the specimen on a universal testing machine (AG-X plus, Shimadzu, Kyoto, Japan) at a constant crosshead speed of 1 mm/min. The biaxial flexural strength (BFS) was then calculated.

After the BFS test, two to three large fragments (those spanning from the center to the edge of the disc) were randomly selected from the six or twelve total specimens, embedded in methacrylic resin (Unifast II, GC), and subjected to argon ion milling using an HITACHI IM3000 Flat Milling System at an accelerating voltage of 2 kV for 5 min. Following ion milling and coating with platinum-palladium (Pt-Pd), each specimen was observed under a field-emission scanning electron microscope (FE-SEM; SU-70, HITACHI, Tokyo, Japan) at a magnification of 15,000 × . SEM images were acquired from 20 randomly selected areas, avoiding polishing marks and covering various regions of the surface.

2.4. Training data preparation

A total of 200 SEM images were obtained and binarized (crystals: white, glass matrix: black) by using Image J software (NIH) according to a threshold of 150. Persistent homology analysis was then performed to extract the topological features underlying the SEM images. This analysis first involves the following steps:

1. Each binarized image was transformed into a persistent diagram using HomCloud library (Ver. 4.6.0), where the scattered data points in the diagram represent topological features.
2. The scattered points from each diagram were vectorized using weight functions.
3. Since the obtained vectors were too large to serve as input data for developing a machine learning model, principal component analysis (PCA) was applied to reduce the dimensionality of the vectors for each product.

After dimensionality reduction, the resulting vectors were referred to

as principal components. Additionally, Bayesian optimization was conducted to determine the appropriate number of principal components. The selected principal components, along with biaxial flexural strength values, were then used as input training data for the machine learning model.

2.5. Machine learning model development and evaluation

Gaussian Mixture Regression (GMR) [26] was employed to develop a machine learning model for predicting biaxial flexural strength. The dataset was divided into training and testing subsets (8:2). The hyperparameters of the model were selected and optimized based on the Bayesian Information Criterion (BIC). To assess the regression accuracy of each model, the coefficient of determination (R^2 value), root mean square error (*RMSE*), and mean absolute error (*MAE*) were calculated.

2.6. Inverse prediction

For inverse analysis validation, Celtra Duo (lowest BFS) and LH052 (highest BFS) were excluded. The range of 390–640 MPa was then selected to reflect the variability among the remaining products while ensuring representative coverage for model testing. An inverse analysis was conducted using the constructed machine learning model. Unlike the direct prediction of the biaxial flexural strengths, predefined biaxial flexural strength values (390, 411, 442, 478, 515, 564, 597, 610, and 640 MPa) were used as input data. PCA was then applied to facilitate the inverse transformation, converting input strength values into vectors and subsequently transforming these vectors into persistent diagrams. Following PH analysis, the projection of significant region onto SEM images for each product was obtained as the output. The overall process is summarized in Fig. 1.

3. Results

Representative SEM images of each lithium disilicate glass-ceramic were shown in Fig. 2. The BFS values of each lithium disilicate glass-ceramics are summarized in Table 1. The extracted topological features were reduced ten principal components (Fig. 3). The ML model was selected and optimized based on the BIC. The maximum BIC value of −1086.2 was achieved at the 22nd iteration (Fig. 4). Using the constructed machine learning model, BFS values were predicted with a test accuracy of 72 % (R^2-*value*: 0.909, *RMSE*: 30.465 MPa, *MAE*: 15.056 MPa) (Fig. 5).

The inversely predicted images of Celtra Duo (BFS=390 MPa) and LH052 (BFS=610 MPa) are shown in Fig. 6 and Fig. 7, respectively.

4. Discussion

The MI approach, an AI-driven materials design method, was employed to predict the BFS value of lithium disilicate glass-ceramics from SEM images. Additionally, geometrically significant regions were successfully overlaid onto SEM images based on predefined biaxial flexural strength values.

Through ion milling treatment, nearly perfectly planar cross-sections of the samples were obtained. If the centroid positions of the crystals within these cross-sections can be accurately extracted using AI techniques of the instance segmentation such as YOLACT [27] or YOLACT++ [28], it is anticipated that topologically invariant features can be identified at least within the two-dimensional plane using PH analysis.

In this study, binarized SEM images were used as input data for PH analysis, ensuring the accessibility of the accumulated data. If SEM imaging is performed repeatedly along the depth direction after ion milling treatment, enabling the three-dimensional reconstruction of crystal morphology and the accurate extraction of crystal centroid positions, it is expected that topologically invariant features could also be
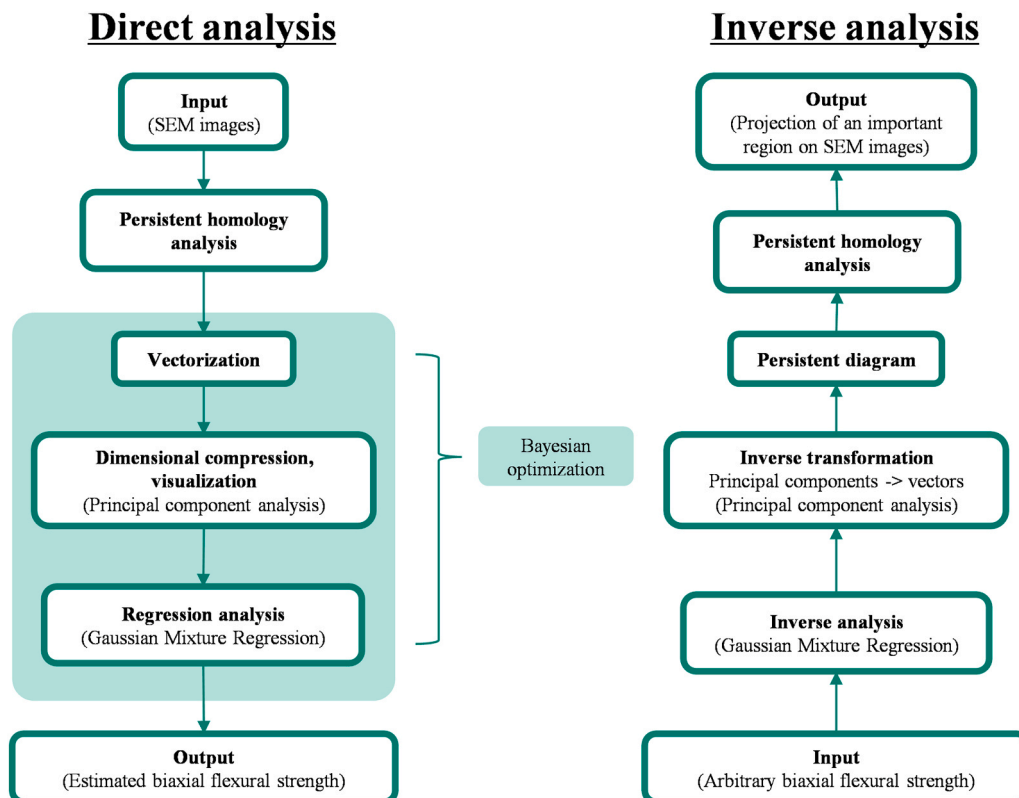

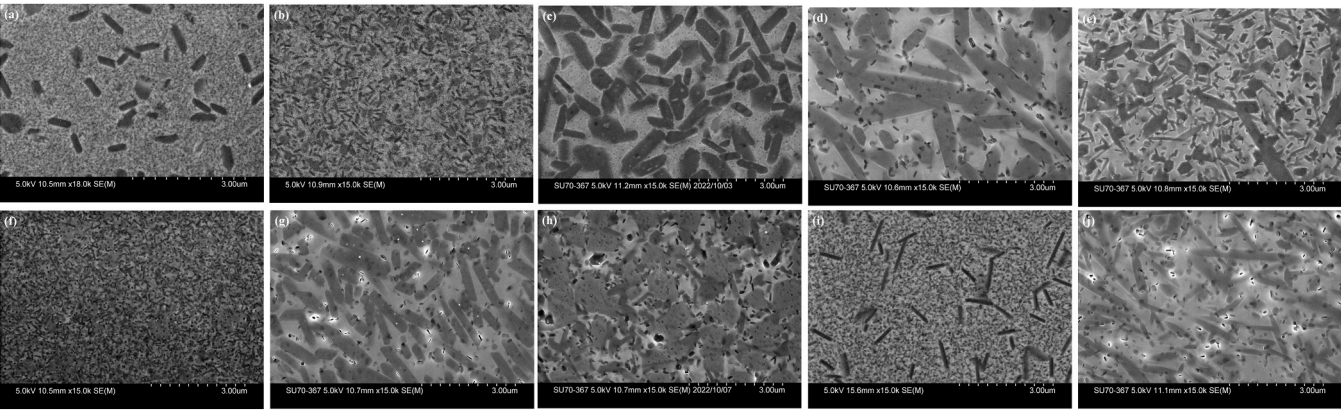**Fig. 1.** Flowchart from direct analysis to inverse analysis.

Fig. 2. Representative SEM images of each lithium disilicate glass-ceramic. (a) Celtra Duo, (b) CEREC Tessera, (c) IPS e.max CAD, (d), IPS e.max Press, (e) LH052, (f) Initial LiSi Block, (g) Initial LiSi Press, (h) N!ce, (i) Sprinity, (j) Vintage Prime Press.

Table 1

In vitro biaxial flexural strengths of ten commercially available/experimental lithium disilicate glass-ceramics.

No.	Glass ceramics	Lot	Shade	BFS (MPa)
1	Celtra Duo	16001012	CT-A3	298 ± 93
2	CEREC Tessera	16009642	MT-A2	543 ± 81
3	IPS e.max CAD	Y08938	LT A3	495 ± 67
4	IPS e.max Press	X49004	LT A2	438 ± 37
5	LH052	211222	n/a	690 ± 92
6	Initial LiSi Block	2010121	A2HT	408 ± 49
7	Initial LiSi Press	1806021	LT A2	508 ± 55
8	N!ce	NJ372	LT A1	432 ± 35
9	Sprinity	36211	A2-T	354 ± 46
10	Vintage Prime Press	521101	HT-A2	542 ± 70

Fig. 4. Bayesian information criterion (BIC).

Fig. 3. Cumulative contribution rate by principal component analysis.

Fig. 5. Regression plot between experimental biaxial flexural strength and estimated biaxial flexural strength (MPa).

identified in three dimensions.

A GMR model was deployed, and the regression plot obtained from the test data showed larger errors, particularly on the high-intensity side. This discrepancy could be attributed to the limited availability of high-intensity data in the input dataset used to train the regression model [26]. These errors are expected to be reduced by incorporating additional high-intensity data. This can be achieved by refining the
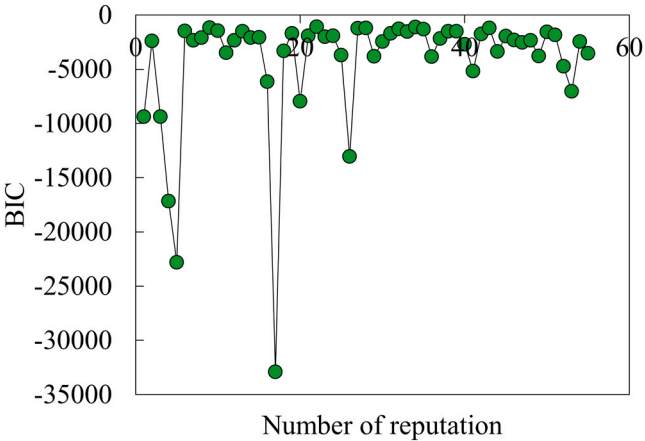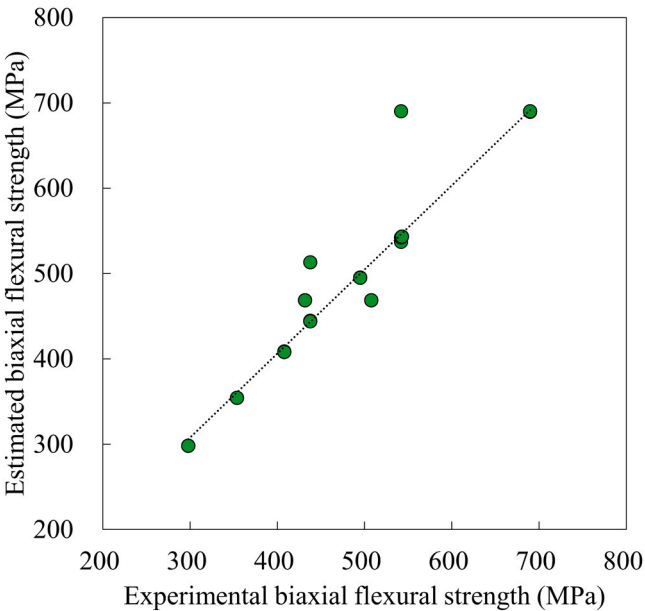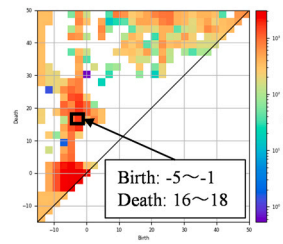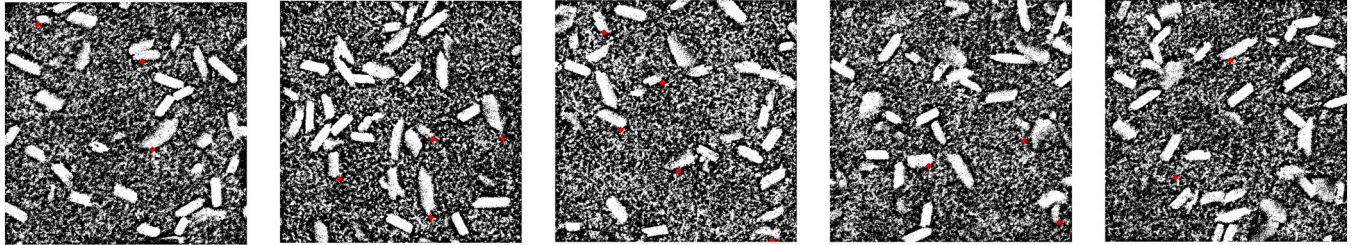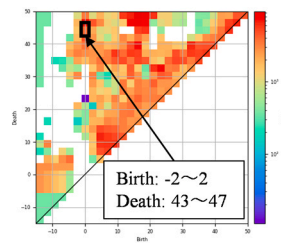
Biaxial flexural strength < **390 MPa**

Fig. 6. Persistent diagram illustrated from arbitrary biaxial flexural strength of 390 MPa and topological features (red dots) overlaid onto binarized SEM images (Celtra Duo).
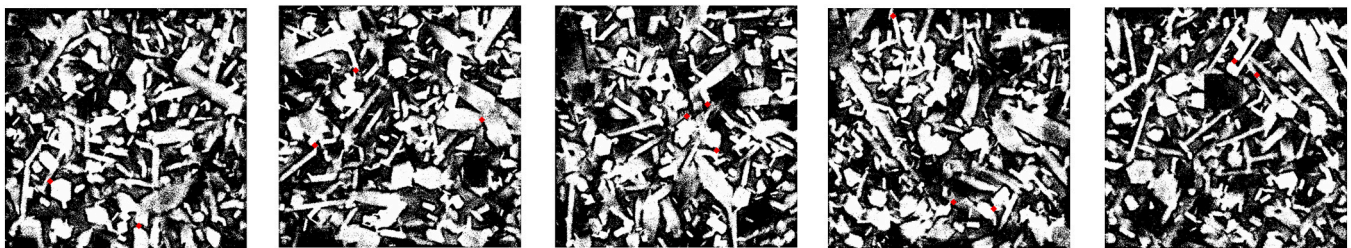

Biaxial flexural strength = **610 MPa**

Fig. 7. Persistent diagram illustrated from arbitrary biaxial flexural strength of 610 MPa and topological features (red dots) overlaid onto binarized SEM images (LH052).

selection of the next prototype candidates based on the regression model's proposed phase-geometrically invariant features, which are designed to achieve the desired material properties identified through inverse analysis.

The inverse analysis of the regression model developed in this study revealed that the boundaries between crystals, as well as those between crystals and the glass matrix, play a crucial role in the development of high-strength lithium disilicate glass-ceramics. This could enable more conservative preparations, reduce the need for opaque substructures,

and simplify laboratory workflows, ultimately benefiting both clinicians and patients. Observing these boundaries using atomic force microscopy or transmission electron microscopy is expected to provide novel insights, facilitating the development of entirely new lithium disilicate glass-ceramics. Apel et al. clarified that microcracks in lithium disilicate glass-ceramics propagate exclusively within the glassy matrix (intragranular), whereas in leucite and apatite glass-ceramics, crack propagation occurs transgranularly and along grain boundaries, respectively [29]. Their findings suggest that a chemical concentration gradient may

potentially be present at the interface between lithium disilicate crystals and the surrounding glass matrix. The distinct interface revealed by hydrofluoric acid etching implies compositional differences between the lithium disilicate crystals and the surrounding glass matrix, which may reflect an underlying chemical concentration gradient [30,31].

To further improve the fracture resistance of lithium disilicate glass-ceramics, several strategies may be considered. Tailoring the chemical composition near the crystal–glass interface could enhance crack deflection mechanisms by amplifying compositional gradients that hinder crack propagation. This may be achieved through controlled diffusion of mobile ions such as Li^+, K^+, or P^{5+} during nucleation and crystallization stages [30,32]. Increasing the degree of crystal interlocking by optimizing the aspect ratio and orientation of lithium disilicate crystals may promote a more tortuous crack path, thereby increasing the energy required for fracture [33]. Engineering residual compressive stresses at the interface through thermal expansion mismatch or phase transformation can act as a barrier to crack advancement [34,35]. Incorporation of nanocrystalline secondary phases or interface modifiers, such as ZrO_2 or Al_2O_3, could serve to reinforce the boundary regions and further suppress crack initiation [32,33]. Collectively, these approaches aim to enhance the structural integrity of lithium disilicate glass-ceramics while maintaining their excellent esthetic and processing properties. These findings have significant clinical implications. Enhancing the flexural strength of lithium disilicate glass-ceramics can expand their applications beyond anterior and single-unit restorations to include posterior crowns, implant-supported prostheses, and even fixed partial dentures, which are currently dominated by zirconia-based ceramics due to their superior mechanical properties [4]. By improving crack resistance through microstructural and interfacial engineering—such as grain boundary optimization and topological design strategies—lithium disilicate ceramics may provide a viable esthetic alternative in high-stress clinical scenarios [3,4].

In the future, instead of binarized SEM images, the instance segmentation is expected to be utilized to accurately extract the centroid positions of individual crystals. This approach would improve the performance of PH analysis, enabling the capture of truly topologically invariant features with greater fidelity. Persistent homology analysis combined with machine learning successfully distinguished between the glassy and liquid phases by capturing subtle but significant differences in the three-dimensional atomic arrangements during glass formation [36]. In this regard, by extracting the centroid positions of each crystal not only from two-dimensional SEM images but also from a three-dimensional volume model reconstructed from images obtained through iterative ion milling in the depth direction, the identification of genuinely topologically invariant features is anticipated.

This extension to 3D not only enhances the topological fidelity but also opens the possibility of correlating specific spatial configurations—such as interfacial curvature, grain boundary networks, and crystal connectivity—with mechanical outcomes [37]. Persistent homology applied to 3D reconstructed volumes may allow for the identification of structural motifs that are otherwise invisible in 2D sections [38]. These motifs, once correlated with mechanical performance through inverse machine learning, can guide the design of new lithium disilicate formulations with targeted strength characteristics [39]. For example, identifying regions of high interfacial tortuosity or dense crystal clustering may inform compositional or thermal processing strategies that promote such features in practice.

5. Conclusion

The inverse analysis established in this study successfully predicted the topological features on SEM images of lithium disilicate glass-ceramics based on biaxial flexural strength values. The ML approach, combined with the inverse analysis, has the potential to significantly enhance the efficiency of developing lithium disilicate glass-ceramics, enabling a more time-efficient method than the traditional

experimental approaches.

Declaration of Competing Interest

Acknowledgements

Data availability

As LH052 is an experimental material, the dataset is not available without prior approval from GC Corporation.

References

[1] Guess PC, Stappert CF, Strub JR. Preliminary clinical results of a prospective study of IPS e.max Press- and cerec ProCAD- partial coverage crowns. Schweiz Mon Zahnmed 2006;116:493–500.

[2] Chen YN, Yeung AWK, Pow EHN, Tsoi JKH. Current status and research trends of lithium disilicate in dentistry: a bibliometric analysis. J Prosthet Dent 2021;126:512–22.

[3] Hallmann L, Ulmer P, Kern M. Effect of microstructure on the mechanical properties of lithium disilicate glass-ceramics. J Mech Behav Biomed 2018;82:355–70.

[4] Zhang Y, Vardhaman S, Rodrigues CS, Lawn BR. A critical review of dental Lithia-Based Glass-Ceramics. J Dent Res 2023;102:245–53.

[5] Strasser T, Wertz M, Koenig A, Koetzsch T, Rosentritt M. Microstructure, composition, and flexural strength of different layers within zirconia materials with strength gradient. Dent Mater 2023;39:463–8.

[6] Borba M, de Araujo MD, Fukushima KA, Yoshimura HN, Cesar PF, Griggs JA, et al. Effect of the microstructure on the lifetime of dental ceramics. Dent Mater 2011;27:710–21.

[7] He WL, Yao CL, Zhao ZH, Rong CR, Zhang YJ, Li B, et al. Optimization of heat treatment program and effect of heat treatment on microstructure and flexural strength of micro-nano-LiSiO whisker-reinforced glass-ceramics. Front Mater 2023;9.

[8] Redwan H, Fan Y, Giordano R, 2nd. Effect of machining damage on the surface roughness and flexural strength of CAD-CAM materials. J Prosthet Dent 2025;133:872–80.

[9] Romanyk DL, Martinez YT, Veldhuis S, Rae N, Guo Y, Sirovica S, et al. Strength-limiting damage in lithium silicate glass-ceramics associated with CAD-CAM. Dent Mater 2019;35:98–104.

[10] Rickman JM, Lookman T, Kalinin SV. Materials informatics: from the atomic-level to the continuum. Acta Mater 2019;168:473–510.

[11] Suwardi A, Wang FK, Xue K, Han MY, Teo PL, Wang P, et al. Machine Learning-Driven biomaterials evolution. Adv Mater 2022;34.

[12] Guo K, Yang ZZ, Yu CH, Buehler MJ. Artificial intelligence and machine learning in design of mechanical materials. Mater Horiz 2021;8:1153–72.

[13] Sun WB, Zheng YJ, Yang K, Zhang Q, Shah AA, Wu Z, et al. Machine learning-assisted molecular design and efficiency prediction for high-performance organic photovoltaic materials. Sci Adv 2019;5.

[14] Tang BJ, Lu YH, Zhou JD, Chouhan T, Wang H, Golani P, et al. Machine learning-guided synthesis of advanced inorganic materials. Mater Today 2020;41:72–80.

[15] Sharma A, Mukhopadhyay T, Rangappa SM, Siengchin S, Kushvaha. Advances in computational intelligence of polymer composite materials: machine learning assisted modeling, analysis and design. Arch Comput Method E 2022;29:3341–85.

[16] Li H, Sakai T, Tanaka A, Ogura M, Lee C, Yamaguchi S, et al. Interpretable AI explores effective components of CAD/CAM resin composites. J Dent Res 2022;101:1363–71.

[17] Paniagua K, Whang K, Joshi K, Son H, Kim YS, Flores M. Dental composite performance prediction using artificial intelligence. J Dent Res 2025. 220345241311888.

[18] Zunger A. Inverse design in search of materials with target functionalities. Nat Rev Chem 2018;2.

[19] Challapalli A, Patel D, Li GQ. Inverse machine learning framework for optimizing lightweight metamaterials. Mater Des 2021;208.

[20] Xia K, Liu X, Wee J. Persistent homology for RNA data analysis. Methods Mol Biol 2023;2627:211–29.

[21] Meng ZY, Anand DV, Lu YP, Wu J, Xia KL. Weighted persistent homology for biomolecular data analysis. Sci RepUk 2020;10.

[22] Edelsbrunner H, Letscher D, Zomorodian A. Topological persistence and simplification. Discret Comput Geom 2002;28:511–33.

[23] Zomorodian A, Carlsson G. Computing persistent homology. Discret Comput Geom 2005;33:249–74.

[24] Kimura M, Obayashi I, Takeichi Y, Murao R, Hiraoka Y. Non-empirical identification of trigger sites in heterogeneous processes using persistent homology. Sci RepUk 2018;8.

[25] Pan ZW, Atila A, Bitzek E, Wondraczek L. Topology of anisotropic glasses from persistent homology analysis. J NonCryst Solids 2024;627.

[26] Shimizu N, Kaneko H. Direct inverse analysis based on Gaussian mixture regression for multiple objective variables in material design. Mater Des 2020;196.

[27] Bolya D, Zhou C, Xiao FY, Lee YJ. YOLACT Real-time instance segmentation. In: 2019 Ieee/Cvf International Conference on Computer Vision (ICCV 2019); 2019. p. 9156–65.

[28] Bolya D, Zhou C, Xiao FY, Lee YJ. YOLACT plus plus better Real-Time instance segmentation. IEEE T Pattern Anal 2022;44:1108–21.

[29] Apel E, Deubener J, Bernard A, Holand M, Muller R, Kappert H, et al. Phenomena and mechanisms of crack propagation in glass-ceramics. J Mech Behav Biomed Mater 2008;1:313–25.

[30] Höland W, Apel E, van 't Hoen C, Rheinberger V. Studies of crystal phase formations in high-strength lithium disilicate glass-ceramics. J NonCryst Solids 2006;352:4041–50.

[31] Poulon-Quintin A, Ogden E, Large A, Vaudescal M, Labrugere C, Bartala M, et al. Chemical surface modification of lithium disilicate needles of a silica-based ceramic after HF-etching and ultrasonic bath cleaning: impact on the chemical bonding with silane. Dent Mater 2021;37:832–9.

[32] Deshpande A.V., Satyanarayana P. Study of Lithium Disilicate Based Nano Glass Ceramics Containing PO. Silicon-Neth. 2022.

[33] Albakry M, Guazzato M, Swain MV. Influence of hot pressing on the microstructure and fracture toughness of two pressable dental glass-ceramics. J Biomed Mater Res B 2004;71b:99–107.

[34] Mackert Jr JR, Twiggs SW, Russell CM, Williams AL. Evidence of a critical leucite particle size for microcracking in dental porcelains. J Dent Res 2001;80:1574–9.

[35] Soares PC, Lepienski CM. Residual stress determination on lithium disilicate glass-ceramic by nanoindentation. J NonCryst Solids 2004;348:139–43.

[36] Hirata A, Wada T, Obayashi I, Hiraoka Y. Structural changes during glass formation extracted by computational homology with machine learning. Commun Mater 2020;1.

[37] Suzuki A, Sasa Y, Kobashi M, Kato M, Segawa M, Shimono Y, et al. Persistent homology analysis of the microstructure of Laser-Powder-Bed-Fused Al-12Si alloy. Mater (Basel) 2023;16.

[38] Thompson EP, Ellis BR. Persistent homology as a heterogeneity metric for predicting pore size change in dissolving carbonates. Water Resour Res 2023;59.

[39] Fang Z, Yan Q. Leveraging persistent homology features for accurate defect formation energy predictions via graph neural networks. Chem Mater 2025;37:1531–40.